# NASA Technical Memorandum 87617

NASA-TM-87617 19860019509

# NONLINEAR DYNAMIC ANALYSIS OF DEPLOYING FLEXIBLE SPACE BOOMS

PAUL E. McGOWAN AND JERROLD M. HOUSNER



SEPTEMBER 1985

NASA
National Aeronautics and Space Administration

**Langley Research Center**
Hampton, Virginia 23665

# NONLINEAR DYNAMIC ANALYSIS OF DEPLOYING FLEXIBLE SPACE BOOMS

by

Paul E. McGowan and Jerrold M. Housner

## SUMMARY

A fundamental investigation of the planar deployment and lock-up of two flexible boom-type appendages which have attached tip masses and are connected to a central rigid body through a rotational spring is presented. Nondimensional parameters are identified and it is shown that, in general, the solution depends only on two mass ratios and one nondimensional stiffness parameter. Results are presented for boom tip deflections, deployment time and root moments at lock-up. A threshold value of the nondimensional stiffness parameter is identified beyond which boom deflections become large. Also, a thorough examination of the effect of nonlinear terms in the equations governing the deployment phase is performed. Nonlinear terms in the deployment equations due to kinematics and structural deformation are required to predict more accurately boom deflections, but retention of an inconsistent set of nonlinear terms leads to erroneous results. In particular, retaining nonlinear kinematic terms while neglecting nonlinear structural terms can produce inaccurate results even below the threshold stiffness value.

## INTRODUCTION

Many space structure designs require the on-orbit deployment of the entire structure or the assembly of various deployable components. The U.S. Space Station for example may be predominantly composed of interconnected deployable subassemblies. Other examples include antenna feed masts, solar arrays, radiators, robotic manipulator arms, and space platforms. Constraints on packaged volume and weight lead to very complex packaging and deployment schemes which require reliability in all phases of the deployment. Since ground testing of many of these concepts may not be practical, dynamic analyses will be relied upon much more than in past projects for verification of deployment concepts.

Two methods proposed for deploying large space structures are extension (or telescoping) and unfolding. Some literature exists on the analysis of extensional deployment (e.g., references 1 - 3). However, as noted in a recent review of dynamic analyses for deploying space structures (reference 4) much less attention has been given to unfolding. This is a shortcoming in deployment analyses because, as proposed space structures grow larger, it is likely that deployment will take place via unfolding or a combination of extension and unfolding. Thus, it is imperative that efficient, verified deployment analyses be developed.

Until recently, much of the research conducted in unfolding deployment has been limited to cases in which the individual elements were assumed to be rigid during deployment (references 5-8). Reference 9, however, presented results of a convected finite element analysis treating the two-dimensional unfolding of slender, flexible beams. This analysis allowed for many interconnected beams and accounted for large rotations and nonlinear deformations. Considerable insight into the behavior of these types of structures was gained; however, the very general nature of the analysis method used makes extensive parameter studies on a computer impractical. Therefore, it is desirable to perform fundamental deployment studies to verify general analysis computer programs, to determine the effect of coupling between nonlinear kinematics and flexiblity, and to gain insight into the unfolding deployment process.

The purpose of this paper is to present results of a fundamental study on the dynamics of deployment, examining the effects of various nonlinear terms arising from different analysis assumptions. The problem used to illustrate these effects is the planar symmetric deployment and subsequent lock-up of two flexible boom-type appendages which are elastically connected to a central rigid body through a rotational spring. The equations of motion are formulated for the deployment and post-lock-up phases and general nondimensional parameters are identified. The deployment phase is analyzed with nonlinear equations, while the post-lock-up phase is analyzed with linear equations. Limiting cases are examined in closed form and the general equations are solved numerically.

Solution accuracy as it pertains to the retention of nonlinear terms is also addressed. Typical results are presented for boom tip deflections, deployment time and peak root bending moments and comparisons are made with results obtained from a finite element deployment code.

## SYMBOLS

| | |
|---|---|
| $c$ | damper coefficient |
| $d$ | vector of problem degrees-of-freedom; $d = (\theta, v/L, w/L)$ |
| $d_m$ | reduced vector of problem degrees-of- freedom when $m_R$ goes to infinity; $d_m = (\theta, w/L)$ |
| $d_r$ | reduced vector of problem degrees-of-freedom when boom is assumed to be rigid; $d_r = (\theta, v/L)$ |
| $D$ | damping matrix |
| $E$ | Young's modulus |
| $f_j$ | jth approximation to the vector of nonlinear terms given by eq. (4a) |
| $F$ | vector of external force |

| | |
|---|---|
| $g_i$ | ith component of the vector of nonlinear kinematic and structural forces from eq. (3); i=1, 2, 3, 4 |
| $H_l$ | dimensional inertial coefficients which are functions of $m_R$ and $m_T$ as provided in the Appendix; l=1,...,6 |
| I | boom cross-sectional area moment of inertia |
| $I_{vv}, I_{ww}, I_{\theta v}$ | nondimensional inertial terms which are $I_{vw}, I_{\theta w}$, functions of $m_R$ and $m_T$ as provided in the Appendix |
| k | nondimensional stiffness parameter, $k = \frac{\bar{k}L}{EI}$ |
| $\bar{k}$ | dimensional rotational spring constant |
| K | nondimensional linear stiffness matrix |
| L | boom length |
| $\bar{m}_B$ | mass of boom |
| $\bar{m}_R$ | one half the root mass |
| $\bar{m}_T$ | tip mass |
| $m_R$ | $\bar{m}_R/\bar{m}_B$ |
| $m_T$ | $\bar{m}_T/\bar{m}_B$ |
| M | mass matrix |
| $M_R$ | bending moment at boom root |
| P | average axial load along the boom due to centrifugal acceleration |
| s | nondimensional coordinate along the boom |
| T | applied moment at boom root due to rotational spring and viscous damper |
| t | time |
| u | axial displacement of boom tip as shown in figure 2 |
| U | axial displacement along the boom as shown in figure 2 |
| v | vertical motion of the boom root as shown in figure 2 |
| w | transverse deflection of the boom tip as shown in figure 2 |
| W | transverse deflection along the boom as shown in figure 2 |

$x,y$ orthogonal axis system shown in figure 2

$\omega_p$ rigid boom pendulum frequency,

$$\omega_p^2 = \frac{\bar{k}}{\left[\bar{m}_T + (1/3)\bar{m}_B\right]L^2}$$

$\omega_1, \omega_2$ nondimensional frequencies given by eqs. (12) and (13)

$\omega_\theta, \omega_v, \omega_w$ uncoupled vibration frequencies given in eq. (6)

$\Omega$ $\omega_1/\omega_2$

$\theta$ rotational degree-of-freedom as shown in figure 2

$\tau$ nondimensional time = $t\omega_p$

$\tau_D$ nondimensional deployment time at which $\theta=\pi/2$

$\tau_{Dr}$ value of $\tau_D$ for a rigid boom

$\xi,\eta$ displacements parallel to the x and y axes respectively

$\zeta$ critical damping ratio in pendulum mode, $\zeta = \frac{c\,\omega_p}{2\sqrt{\bar{k}}}$

## ANALYSIS

The planar unfolding deployment of two boom-type appendages which have attached payloads and are connected to a central rigid body through a rotational spring is depicted in fig. 1. Assuming symmetric deployment, the mathematical model of fig. 1b is applicable. The deployment mechanism consists of a linear prestressed rotational spring, which drives the deployment and is at its neutral positon at lock-up, and a linear rotational viscous damper which can be used to control the motion during deployment. Thus, the applied moment at the root during deployment is

$$T = \bar{k}(\pi/2-\theta) - c\dot{\theta}$$

where $\bar{k}$ is the rotational spring constant and c is the rotational viscous damping constant. When the boom root has deployed through a 90 degree angle the root joint is assumed to lock-up and become perfectly rigid (herein referred to as lock-up), and the boom vibrates in the post-lock-up phase as depicted in fig. 1b.

The analysis presented herein is divided into two parts, a deployment phase and a post-lock-up phase. The solution of the deployment phase provides the intial conditions for the post-lock-up phase.

## Deployment Phase

The motion and deformation of the boom , (see fig. 2), may be described by $\theta$, the rotation of the boom root; v/L, the nondimensional translation of the boom root along the y axis; U/L, the axial displacement of the boom along its length; and w/L, the transverse deflection of the boom along its length. Also shown in fig. 2 are u, the axial displacement of the boom tip and w, the transverse deflection of the boom tip.

The equations of motion describing the deployment phase (i.e., from rest, $\theta=0$, to lock-up, $\theta=\pi/2$) are highly nonlinear due to the presence of kinematic centrifugal and Coriolis forces , the large angle rotation terms inherent in the mass matrix and the moderate deformations of the boom. An approximate solution to these equations may be found by assuming that the transverse boom deflection, W, and the axial boom deflection, U, have cubic and linear variations respectively along the boom; that is,

$$W(s)=ws^2(3-s)/2 \quad ; \quad U(s)=us \tag{1}$$

where s is a nondimensional coordinate along the boom, going from zero at the root to one at the tip, w is the value of W(1) and u is the value of U(1).

In addition, axial deflections of the boom may be eliminated by imposing the simplifying assumption that the boom is inextensional. To first order nonlinear terms, this implies that the average strain over the boom length is zero and yields,

$$u/L = -(3/5)(w/L)^2 \tag{2}$$

As a consequence of eqs. (1) and (2), the vector d containing the reduced system degrees-of-freedom has three entries, namely,

$$d = \begin{Bmatrix} \theta \\ v/L \\ w/L \end{Bmatrix}$$

Then the equations of motion governing the deployment phase may be expressed in the form,

$$M\ddot{d} + D\dot{d} + Kd + \sum_{i=1}^{4} g_i = F \tag{3}$$

where the initial conditions on d and $\dot{d}$ are zero, and where M, D and K are the mass, dissipation and stiffness matrices,respectively, the sum of the $g_i$'s is the vector of nonlinear kinematic and structural forces and F is the vector of external forces. The derivation of M, D, K, $g_i$ and F is provided in the Appendix.

The matrices M, D, and K are given by,

$$M = \begin{bmatrix} 1 & -I_{\theta v}\sin\theta & -I_{\theta w} \\ -I_{\theta v}\sin\theta & I_{vv} & I_{vw}\sin\theta \\ -I_{\theta w} & I_{vw}\sin\theta & I_{ww} \end{bmatrix}$$

$$D = \begin{bmatrix} 2\zeta & 0 & 0 \\ 0 & 0 & 0 \\ 0 & 0 & 0 \end{bmatrix}$$

$$K = \begin{bmatrix} 1 & 0 & 0 \\ 0 & 0 & 0 \\ 0 & 0 & 3/k \end{bmatrix}$$

where $I_{ww}$, $I_{vv}$, $I_{vw}$, $I_{\theta w}$ and $I_{\theta v}$ are nondimensional inertial properties, given in the Appendix, involving only the ratios of the tip mass and root mass to the boom mass, and k is a nondimensional stiffness parameter defined as,

$$k = \frac{\bar{k}L}{EI}$$

Also, $\zeta$ is the percent of critical damping in the pendulum mode of the boom due to the presence of the linear viscous damper at the boom root

$$\zeta = \frac{c\,\omega_p}{2\sqrt{\bar{k}}}$$

and $\omega_p$ is the pendulum frequency of a rigid boom with a rotational spring and pin at its root, namely,

$$\omega_p^2 = \frac{\bar{k}}{[\bar{m}_T + (1/3)\bar{m}_B]L^2}$$

The complete nonlinear force vector in eq. (3) contains many nonlinear kinematic and structural terms. In order to assess the importance of these terms the following approximations to this vector are introduced,

$$f_j = \sum_{i=1}^{j} g_i \; ; \; j=1,\ 2,\ 3,\ 4 \qquad (4a)$$

where each of the $f_j$ represent varying levels of approximations to the complete nonlinear force vector, and each of the $g_i$ are given in the appendix. These approximation levels correspond to various assumptions that have been used in the past by different investigators.

When considering only the nonlinear terms arising from purely kinematic considerations of a flexible boom, the first approximate force vector $f_1$ may be written as,

$$f_1 = \begin{Bmatrix} I_{vw}(w/L)(\ddot{v}/L)\cos\theta \\ \left[I_{vw}\{\ddot{\theta}(w/L)\cos\theta - \dot{\theta}^2(w/L)\sin\theta + 2\dot{\theta}(\dot{w}/L)\cos\theta\} - I_{\theta v}\dot{\theta}^2\cos\theta\right] \\ -I_{ww}(w/L)\dot{\theta}^2 \end{Bmatrix} \qquad (4b)$$

where in this equation all terms involving products of the boom transverse deflection have been neglected. This order of approximation is equivalent to that used in ref. 10.

When the deflection terms which were neglected in eq. (4b) are included, the force vector $f_2$ takes the form

$$f_2 = f_1 + \begin{Bmatrix} \left[I_{ww}\{(w/L)^2\ddot{\theta} + 2(w/L)(\dot{w}/L)\dot{\theta}\}\right] \\ 0 \\ 0 \end{Bmatrix} \qquad (4c)$$

This order of approximation is the one most often used when nonlinear effects are included; i.e., a linear structural representation is used, often in the form of a summation of modes, and the resulting nonlinear kinematic terms are retained.

The next level of approximation to the force vector is obtained by including differential stiffness along with the nonlinear kinematic terms of eq. (4c), thus, $f_3$ is written as,

$$f_3 = f_2 + \begin{Bmatrix} 0 \\ 0 \\ (6/5)(w/L)\dot{\theta}^2 \end{Bmatrix} \qquad (4d)$$

where the differential stiffness effect is the term in the third row of the vector added to $f_2$.

As a final level of approximation, when along with the nonlinear kinematic and differential stiffness terms, a complete set of first-order nonlinear structural terms are retained, the nonlinear force vector, $f_4$, is defined. In accordance with eq. (4a), $f_4$ is assembled using eqs. (A7) through (A10) in the Appendix.

The effects of the various levels of approximations to the nonlinear force vector on the solution accuracy are examined in a later section.

Also from eq. (3), the vector F in dimensionless form may be expressed as,

$$F = \begin{Bmatrix} \pi/2 \\ 0 \\ 0 \end{Bmatrix}$$

Furthermore a dot (.) as used in eq. (3) indicates differentiation with respect to a dimensionless time parameter, $\tau$, which is related to time t as,

$$\tau = \omega_p t \tag{5}$$

An examination of eq. (3) reveals that, for given values of root and tip mass to boom mass ratios, only one parameter, namely k, is required to determine the nondimensional vector d.

Equation (3) may be solved by direct numerical integration using any of a large selection of explicit integrators. In addition, certain limiting cases of eq. (3) may be solved in closed form when the nonlinear force vector is neglected, such as when eq. (3) is an uncoupled set, when the boom is rigid and when the root mass is very large. Each of these limiting cases is discussed in the following sections.

Uncoupled Equations - Equation (3) represents a coupled set of equations. Coupling is provided through the mass matrix and through the nonlinear force vector. If it is assumed that eq. (3) can be approximated as an uncoupled set of three equations, the nondimensional natural vibration frequencies with nonlinear terms neglected are,

$$\omega_\theta = 1$$

$$\omega_v = 0$$

$$\omega_w = \sqrt{3/k} \tag{6}$$

where $\omega_\theta$ is associated with the pendulum mode of a rigid boom, $\omega_w$ is associated with the fundamental cantilever boom frequency since the deflection W(s) has been chosen such that its gradient is zero at the root, and $\omega_v$ is associated with the rigid body freedom of the system in the v direction. The dimensional frequencies are found by multiplying the nondimensional frequencies by $\omega_p$.

Rigid Boom - Equation (3) may be readily reduced to the limiting case of a rigid boom. This is accomplished by setting w to zero and striking the third row and column of M, D, and K, and the third row of F. Note that the nonlinear force vector vanishes when the boom is treated as rigid. The resulting equation is

$$\begin{bmatrix} 1 & -I_{\theta v}\sin\theta \\ -I_{\theta v}\sin\theta & I_{vv} \end{bmatrix} \ddot{d}_r + \begin{bmatrix} 2\zeta & 0 \\ 0 & 0 \end{bmatrix} \dot{d}_r + \begin{bmatrix} 1 & 0 \\ 0 & 0 \end{bmatrix} d_r = \begin{Bmatrix} \pi/2 \\ 0 \end{Bmatrix} \tag{7}$$

where,

$$d_r = \begin{Bmatrix} \theta \\ v/L \end{Bmatrix}$$

As revealed by eq. (7), all nondimensional results are independent of the rotational spring constant, $\bar{k}$. For example, as the root mass goes to infinity, (or equivalently v goes to zero), $\theta$ limits to $\theta_r$, where

$$\theta_r = (\pi/2)\left[1 - e^{-\zeta\tau}\cos\tau\sqrt{1-\zeta^2}\right]$$

and the nondimensional deployment time , $\tau_D$ (the time to achieve lock-up, $\theta=\pi/2$) limits to $\tau_{Dr}$, where

$$\tau_{Dr} = \frac{\pi}{2\sqrt{1-\zeta^2}} \tag{8}$$

Infinite Root Mass - Equation (3) may also be reduced to the limiting case of an infinite root mass or equivalently to the case of a constrained boom root in the v direction. This is accomplished by striking the second row and column of M, D, and K and the second row of F. The resulting equation is,

$$\begin{bmatrix} 1 & -I_{\theta w} \\ -I_{\theta w} & I_{ww} \end{bmatrix} \ddot{d}_m + \begin{bmatrix} 1 & 0 \\ 0 & 3/k \end{bmatrix} d_m = \begin{Bmatrix} \pi/2 \\ 0 \end{Bmatrix} \tag{9}$$

where,

$$d_m = \begin{Bmatrix} \theta \\ w/L \end{Bmatrix}$$

and where the damper and nonlinear terms of eq. (3) have been neglected.

The solution of eq. (9) is

$$\theta = (\pi/2)\{1 - b\cos\omega_1\tau - (1-b)\cos\omega_2\tau\} \tag{10}$$

$$w/L = -\frac{\pi}{2I_{\theta w}}\left[b\frac{\omega_2^2 - 1}{\omega_1^2}\cos\omega_1\tau + (1-b)\frac{\omega_2^2 - 1}{\omega_2^2}\cos\omega_2\tau\right] \tag{11}$$

where,

$$\omega_1^2 = \frac{1}{2(I_{ww} - I_{\theta w}^2)}\left[I_{ww} + \left(\frac{3}{k}\right) - \sqrt{\left(I_{ww} - \frac{3}{k}\right)^2 + \frac{12}{k}I_{\theta w}^2}\right] \tag{12}$$

$$\omega_2^2 = \frac{1}{2(I_{ww} - I_{\theta w}^2)}\left[I_{ww} + \left(\frac{3}{k}\right) + \sqrt{\left(I_{ww} - \frac{3}{k}\right)^2 + \frac{12}{k}I_{\theta w}^2}\right] \tag{13}$$

$$b = \frac{\omega_1^2 - \Omega^2}{1 - \Omega^2}$$

and ,

$\Omega = \omega_1/\omega_2$

Shown in fig. 3 are the variations with k of $\omega_1$ and $\omega_2$. Equation (9) indicates that these frequencies reflect the coupling of the $\theta$ and w degrees-of-freedom through the mass matrix. The effects of this coupling on the solution can be seen from fig. 4, which depicts the root rotation $\theta$ versus the nondimensional time, $\tau$ for flexible booms with two values of the stiffness parameter k. Also shown in fig. 4 is the $\theta$ history for a rigid boom (recall that this is independent of k). Both curves of fig. 4 for k=0.10 and k=0.90 exhibit the oscillatory motion of $\theta$, however, the number of oscillations for the two cases are very different since the $\omega_2$ frequency from fig. 3 associated with the k=0.90 case is much lower than that of the k=0.10 case. Furthermore, as k increases, the degree of coupling between $\omega_1$ and $\omega_2$ increases such that the solution for $\theta$, and hence the deployment time, changes.

Provided the amplitude of the oscillations associated with $\omega_2$ are small, the nondimensional deployment time is essentially $\pi/2$. However, as boom deformation increases, the amplitude of these oscillations increases and as can be envisioned from fig. 3, the deployment time can change abruptly as the boom locks up due to these oscillations.

Referring again to fig. 3, the coupled nondimensional frequency $\omega_1$ limits to $\omega_\theta$ as the stiffness parameter k goes to zero, (i.e., the rotational spring stiffness vanishes or the boom becomes rigid), and limits to the cantilever boom frequency, $\sqrt{3/k}$ as k approaches infinity, (i.e., the boom root becomes cantilevered or the boom stiffness vanishes). Since $\omega_1$ is very close to $\omega_\theta$ for k less than about one, it is natural to refer to $\omega_1$ as the coupled pendulum frequency.

For small values of k, the coupled frequency $\omega_2$ limits to $\omega^*\sqrt{3/k}$ and for large values of k limits to $\omega^*$ where,

$$\omega^* = [I_{ww}/(I_{ww}-I_{\theta w}^2)]^{1/2}$$

If the tip mass to boom mass ratio were allowed to approach infinity, $\omega_2$ would approach the nondimensional frequency of a beam with a rotational spring at the root and a simple support at the tip, and if in addition, k were allowed to go to zero, $\omega_2$ would approach the nondimensional frequency of a simply supported beam. It is thus reasonable to associate $\omega_2$ with boom flexure.

### Post-Lock-Up Phase

The solution of eq.(3) at $\tau = \tau_D$ provides the initial conditions for the post-lock-up analysis. Whereas the deployment phase is analyzed with nonlinear equations, the post-deployment phase is analyzed with linear equations with nonlinear initial conditions on W and $\dot{W}$. It is solved herein using modal superposition where the modes of a beam with a guided root and masses at each end are used. In terms of the nondimensional parameters used herein, the beam equation for the post-lock-up phase is,

$$W_{,ssss} + [k/(1/3 + m_T)]\ddot{(W)} = 0 \qquad (14)$$

with boundary conditions,

$$W_{,sss}(0) = (1/2)m_R k\ddot{W}(0)/[(1/3)+m_T]$$

$$W_{,s}(0) = 0$$

$$W_{,ss}(1) = 0$$

$$W_{,sss}(1) = -(1/2)m_T k\ddot{W}(1)/[(1/3)+m_T]$$

where, $m_T$ and $m_R$ are the ratios of the tip mass and root mass, respectively, to the boom mass.

## DISCUSSION OF RESULTS

### Accuracy

The accuracy of the equations of motion (3) is considered in this section. Accuracy is especially important in the deployment phase which is analyzed with nonlinear equations. The nonlinear terms arise from boom flexure and enter the equations of motion through both kinematic and structural considerations. It is often difficult for the analyst to decide which nonlinear terms should be retained in the analysis so as to generate a consistent formulation which produces accurate results. When, as is often desirable, the nonlinear equations of motion are linearized about a given state in order to assess stability, an inconsistent set of nonlinear terms retained in the equations can lead to erroneous results.

Accuracy of deployment time, $\tau_D$, (which is a measure of the accuracy in computing $\theta$), and transverse deflection of the boom tip at lock-up, w/L, are examined for the case of the root mass to boom mass parameter, $m_R$, approaching infinity and the tip mass to boom mass parameter, $m_T$, equal to 1.0. It is anticipated that the general conclusions for this case are also valid for other values of $m_R$ and $m_T$.

Discussion of accuracy is divided into two parts. First, in figs. 5a and 6a the solutions given by the linearized equations of motion (nonlinear force vector neglected) and the equations of motion with the nonlinear force vector (given by $f_4$) employed are compared to the exact solution taken as the converged finite element results of ref. 9. Second, various levels of

approximations to the nonlinear solution as given by $f_1$ through $f_4$ are compared in figs. 5b and 6b.

Comparison of Linear and Present Nonlinear Solutions to Exact Solution - The exact, linear and present nonlinear solutions are referred to and discussed as follows:

(1) Exact nonlinear kinematics/exact nonlinear structure
(2) Linear kinematics/linear structure
(3) Exact nonlinear kinematics/approximate nonlinear structure, $f_4$

Exact nonlinear kinematics/exact nonlinear structure - The converged results from the general finite element nonlinear deployment code of ref. 9 are taken to be exact. This program allows for unlimited deformations and rotations with the assumptions herein relaxed.

Figure 5a displays the variation in the nondimensional deployment time, $\tau_D$, with the nondimensional stiffness parameter, k. Increasing values of k can be interpreted as either increasing the value of the rotational spring constant or as decreasing the bending stiffness of the boom. Similarly, fig. 6a displays the variation in the boom tip deflection at lock-up, w/L, with k.

For small values of k the deployment time is approximately that of the rigid boom case, $\tau_{Dr}=\pi/2$; however, as k increases a threshold value is reached, near one, at which the deployment time decreases rapidly. As k approaches infinity the deployment time goes to zero. In addition, as k increases beyond the threshold value the boom tip deflection of fig. 6a also increases and limits to L as k approaches infinity; i.e., no axial extension of the boom occurs. Sketches of the boom's deformed shape at lock-up are provided in fig. 6a to allow the reader to visualize what occurs to the physical boom as k is increased.

Linear kinematics/linear structure - The solution for $\theta$ and w when only linear terms are retained is given by eqs. (10) and (11). The deployment time $\tau_D$ is found from the transcendental equation which results from setting $\theta$ to $\pi/2$ in eq. (10). Also shown in figs. 5a and 6a is the variation of $\tau_D$ and w/L with the nondimensional stiffness for this solution.

The value of $\tau_D$ depends on $\omega_1$, associated with pendulum motion of the boom, and $\omega_2$, associated with flexural vibration of the boom. Recall from fig. 3, that at small values of k, $\omega_2$ is much higher than $\omega_1$ and thus does not couple with $\omega_1$ to affect deployment time. Consequently, the linear solution from fig. 5a is very close to the rigid boom pendulum deployment time ($\tau_{Dr}=\pi/2$) when k is small, as was the exact solution. Furthermore, as shown in fig. 6a, the boom tip deflection magnitude at lock-up is small provided k is small. As the value of k increases, however, the two modes associated with $\omega_1$ and $\omega_2$ couple together. This coupling appears to produce the threshold dropoff noted with the exact solution. For k above the threshold value of about one, the deployment time decreases rapidly to a value of about 0.2, (the linear equations do not permit the curve to go to

zero as k goes to infinity as in the case of the exact solution), and the tip deflection magnitude as seen in figure 6a gets large; limiting to about 1.6L as k goes to infinity compared to L for the exact solution. Thus the linear equations are in error for predicting tip deflection for very large values of k.

Exact nonlinear kinematics/approximate nonlinear structure, $f_4$ - When, along with linear terms, the nonlinear inertial, differential stiffness and first-order nonlinear structural terms are retained, the nonlinear vector as given by $f_4$ is employed. These nonlinear terms are derived in the Appendix by allowing axial motion of the boom in such a way as to constrain the average axial strain in the boom to vanish to first-order nonlinear terms.

The predicted deployment time and tip deflection magnitude for this solution are also given in figs. 5a and 6a respectively. The results indicate that for very small k the inclusion of the nonlinear terms has little effect and results are close to those of the rigid boom and linear equations solution. For deployment time, this solution also indicates a threshold k value of 1.0 and follows the linear and exact solutions closely. For tip deflection at lock-up, the nonlinear solution approaches a deflection of about 1.25L as k becomes large. This implies that there is still some inaccuracy in computing the boom tip deflection at very large k even though the boom axial strain has been constrained to first-order nonlinear terms, however, the error is considerably less than that given by the linear solution.

In light of these results it appears that a threshold value of k exists beyond which considerable deformation of the boom results and that the linear solution predicts the existence of this threshold. For the case of $m_R$ very large and $m_T$ equal to one, the threshold value is about one. It is expected that results for other mass ratios will exhibit the same character with different threshold values.

Various Approximations to Nonlinear Force Vector, $f_i$ - Consideration is now given to how the various levels of approximations to the nonlinear force vector, eqs. (4a)-(4d), affect the solution accuracy. For comparison, the results from figs. 5a and 6a for the complete nonlinear force vector (exact nonlinear kinematics/approximate nonlinear structure, $f_4$) are repeated on figs. 5b and 6b. Each of the approximations are referred to and discussed as follows:

(1) Approximate nonlinear kinematics/linear structure, $f_1$
(2) Exact nonlinear kinematics/linear structure, $f_2$
(3) Exact nonlinear kinematics/linear structure with differential stiffness, $f_3$

Approximate nonlinear kinematics/linear structure, $f_1$ - When only the nonlinear inertial terms arising from purely kinematic considerations are retained, the nonlinear force vector is given by $f_1$. Some references (e.g. ref. 10) retain only terms of this type by neglecting products of the deformation (w/L), which is assumed small. Curves for deployment time and tip

deflection magnitude at lock-up with the $f_1$ vector employed are given in figs. 5b and 6b respectively.

The results indicate that this level of approximation predicts a considerably lower threshold value of k=0.02 than the linear and nonlinear solutions from fig. 5a. Furthermore as the threshold value of k=0.02 is exceeded, the tip deflection prediction grows without bounds.

Exact nonlinear kinematics/linear structure, $f_2$ - When the kinematic terms which were neglected in obtaining $f_1$ are retained, the force vector is given by $f_2$. Note that the deployment time prediction from fig. 5b for this case peaks at a large value after the threshold value of k=1.0 is exceeded and then rather than dropping to zero levels off to a value higher than the rigid deployment time. In addition, the tip deflection prediction from fig. 6b grows without bounds as the threshold value of k=1.0 is exceeded. Thus, this level of approximation is in poor agreement with the exact results.

The unbounded growth in the tip deflection for the $f_1$ and $f_2$ cases may be traced to the presence of the term in the third row of both vectors. If the boom were rotating at a constant velocity, this term would enter the stiffness matrix of the system as a negative linear term on the diagonal; thus subtracting from the boom bending stiffness. Clearly, for a sufficiently large angular rotation rate, boom deformation would grow without bound.

This physically impossible result occurs due to the neglect of boom stiffening from centrifugal forces which become significant when the angular rate gets large. Examination of this stiffening term shows it to be of the same order of magnitude as the inertial term which is usually retained by analysts and consequently the stiffening term should also be retained.

Exact nonlinear kinematics/linear structure with differential stiffness, $f_3$ When, in addition to the exact nonlinear kinematic terms of $f_2$, differential stiffness is included, the nonlinear force vector is given by $f_3$. From eq. (4d) the coefficient of the term in the third row may be shown from the definitions in the Appendix to always be positive. Thus inclusion of differential stiffness prevents the deformations from growing unboundedly as shown in fig. 6b. The tip deflection magnitude is seen to limit to about 1.2L as k becomes very large. Although there is still some inaccuracy in computing the boom deflection at the upper limit of k, the error has been significantly reduced by the addition of the differential stiffness term.

Also, for k above the threshold value of 1.0 the deployment time from fig. 5b increases somewhat above the rigid boom solution rather than dropping off rapidly as did the linear solution. Therefore, the retention of the differential stiffness term in the w equation improves the prediction of boom tip deflection, yet it still does not yield an accurate prediction of deployment time, which is associated with the $\theta$ equation.

From the foregoing, it thus appears that retaining only some of the nonlinear terms arising in the equations of motion can lead to inconsistent results. This is especially true for the two cases ($f_1$ and $f_2$) when only

the nonlinear inertial terms arising strictly from kinematic considerations are retained.

## Deployment Time

As displayed in fig. 5a, the nondimensional deployment time of a flexible boom, whose value of k is less than the threshold value, is closely approximated by that of a rigid boom. This is generally true independent of whether or not nonlinear terms are retained. Although threshold values for various mass ratios are not provided herein, it is expected that in many applications typical values of k will be quite small and less than the appropriate threshold value. For example, if a rotational spring constant were sized to rotate the upper and lower arm booms of the Space Shuttle RMS (ref. 11) through a 90 degree rotation in 15 seconds while carrying a 32,000 pound payload, the value of k would be 0.10 or one order of magnitude below the threshold value found in figs. 5 and 6. Thus rigid boom deployment times should provide reasonably accurate approximations for typical flexible booms.

Figure 7 displays the deployment times for rigid booms with various values of the two mass ratios. From eq. (7), the dimensionless deployment time $\tau_D$ depends only on the terms $I_{\theta y}$ and $I_{vy}$ which in turn depend only on the two mass ratios. The actual deployment time may be computed via eq. (5) by dividing $\tau_D$ by the pendulum frequency $\omega_p$.

## Effect Of Root Damping

The effects of a rotational viscous damper in the deployment mechanism for controlling rotation rate during deployment is examined in this section. Displayed in fig. 8 is the root rotation history during the deployment phase for the case of k=0.16 and for the same mass ratios used in fig. 5. The curve denoted as the rigid assumption is the solution to eq. (8) and represents the rotation of a rigid boom with 2% damping applied. The solid curve provides the undamped rotation of the boom root accounting for flexibility. This solution is seen to oscillate throughout the deployment due to the boom flexural vibrations associated with the $\omega_2$ frequency from eq. (13). The dashed curve represents the root rotation for a flexible boom with 2% of critical damping added at the boom root. Note that the root damper attenuates the boom flexural vibrations. This effect is due to the strong coupling between rigid body rotation and boom flexure.

## Post Lock-Up Root Moments

Of interest in the post-lock-up phase is the peak root bending moment following lock-up. Shown in the solid curve of fig. 9 is the variation of the peak root moment $M_R$ normalized by EI/L with the nondimensional stiffness parameter k for the same mass ratios used in fig. 5. For these results the range of k was limited to be below the threshold value where the linear and nonlinear solutions are in good agreement and the boom deflections are small.

Also shown by the dashed curve in fig. 9, is the peak lock-up moments under the assumption that the boom remains perfectly rigid during the deployment phase, and then is allowed to become flexible in the post lock-up phase. The trend of the dashed curve shows that the root bending moment is proportional to the square root of the rotational spring constant. The difference in the two curves of fig. 9 indicates that neglect of boom flexibility during deployment leads to nonconservative predictions of root lock-up moments for essentially all values of the stiffness parameter.

## CONCLUDING REMARKS

A fundamental investigation of the planar deployment and lock-up of two flexible boom-type appendages which have attached tip masses and are connected to a central rigid body through a rotational spring has been presented. The equations of motion were formulated for the nonlinear deployment phase and the linear post-lock-up phase. Nondimensional parameters were identified and it was shown that the solution depends only on two mass ratios and one nondimensional stiffness parameter.

Accuracy of the deployment equations was examined through comparison with converged results from a finite element deployment code and a threshold value of the nondimensional stiffness parameter was identified beyond which the boom undergoes large flexural deformations. The linear solution produces accurate deployment times, but beyond the threshold does not produce accurate boom deflections.

For more accurate boom deflection predictions above the threshold value, nonlinear effects need to be included. However, it was shown that great care must be exhibited in retaining nonlinear terms, for an inconsistent choice led to erroneous results even below the threshold value. In particular, the retention of only nonlinear inertial terms derived from purely kinematic considerations can lead to erroneous results. Unfortunately it is only these nonlinear terms which are retained in many analyses. Retention of a complete set of nonlinear terms as derived herein were generally in good agreement with converged results from a general finite element deployment program.

Typical booms have small stiffness parameter values and it was found that for booms with stiffness parameters less than the appropriate threshold value, deployment times are accurately predicted under the assumption of a rigid boom deployment. Deployment times for rigid booms with various mass ratios were presented.

It was found that a damper used to control rotational rate during deployment also suppresses boom flexural vibrations during deployment. This effect is due to the strong coupling between rigid body rotation and flexural deformations.

Results were also presented for post-lock-up peak root bending moments. While the assumption of a rigid boom during the deployment phase led to accurate prediction of deployment times for small stiffness

parameters, the same assumption made in conjunction with allowing flexibility following lock-up led to underpredicting the peak root moments.

## APPENDIX

The equations of motion may be derived using the principle of virtual work,

$$\delta\Gamma_B+\delta\Gamma_S+\delta\Gamma_I+\delta\Gamma_D=0 \tag{A1}$$

where, $\Gamma_B$, $\Gamma_S$, $\Gamma_I$ and $\Gamma_D$ are the energies associated with the boom, the rotational spring, the inertial forces and the damping forces respectively, and $\delta$ is the variational operator.

From ref. 12, the contribution of the internal boom forces to the total virtual work may be expressed as,

$$\delta\Gamma_B = \int_0^1 \{[-\frac{P}{L} W_{,ss} + (\frac{EI}{L})^3 W_{,ssss}]\delta W + P\delta U_{,s}\}ds + \{[\frac{P}{L} W_{,s} + (\frac{EI}{L})^3 W_{,sss}]\delta W\}_{s=1} \tag{A2}$$

where, P represents the average axial load in the boom.

Substituting the assumed deformation shapes of eq. (1) into eq. (A2) yields,

$$\delta\Gamma_B=[\frac{3EI}{L^3} w + \frac{6P}{5L} w]\delta w + P\delta u$$

The contribution of the rotational spring to the total virtual work is,

$$\delta\Gamma_S=(\frac{\pi}{2} -\theta)\bar{k}\delta\theta$$

and that of the damper is,

$$\delta\Gamma_D=c\omega_p\dot{\theta}\delta\theta$$

The contribution of the inertial forces to the total virtual work is,

$$\delta\Gamma_I = \bar{m}_B\omega_p^2 \int_0^1 [\ddot{\eta}\delta\eta + \ddot{\xi}\delta\xi]ds + \bar{m}_T[\ddot{\eta}\delta\eta + \ddot{\xi}\delta\xi]_{s=1} \tag{A3}$$

where,

$$\xi = [sL+U(s)]\sin\theta - W(s)\cos\theta \tag{A4}$$

$$\eta = v + [sL+U(s)]\cos\theta + W(s)\sin\theta \tag{A5}$$

After differentiating eqs. (A4) and (A5) with respect to dimensionless time $\tau$, utilizing the assumed shape functions of eq. (1) and substituting the results into eq. (A3), the virtual work of the inertial forces can be rewritten as,

$$\delta\Gamma_I/(\bar{m}_B\omega_P^2)= \{[H_1L^2+H_2w^2 + H_1uL(2+u/L)]\ddot{\theta} + (H_5w\cos\theta-H_4L\sin\theta)\ddot{v} + 2H_1L(1+u/L)\dot{u}\dot{\theta} - H_3\ddot{w}L(1+u/L) + H_3w\ddot{u} + H_4\ddot{v}u\}\delta\theta$$

$$+ \{-H_1 L\dot{\theta}^2 + H_3 w\ddot{\theta} + H_1 \ddot{u} + 2H_3 \dot{w}\dot{\theta} - H_1 \dot{\theta}^2 u$$
$$+ H_4 \ddot{v}\cos\theta\}\delta u$$
$$+ \{-H_3 L(1+u/L)\ddot{\theta} + H_2 \ddot{w} + H_5 \ddot{v}\sin\theta$$
$$- H_2 w\dot{\theta}^2 - 2H_3 \dot{u}\dot{\theta}\}\delta w$$
$$+ \{(H_5 w\cos\theta - H_4 \sin\theta)\ddot{\theta} + H_5 \ddot{w}\sin\theta + H_6 \ddot{v}$$
$$+ (H_4 \cos\theta - H_5 w\sin\theta)\dot{\theta}^2 + 2H_5 \dot{\theta}\dot{w}\cos\theta$$
$$+ H_4 [u(\ddot{\theta}\sin\theta + \dot{\theta}^2\cos\theta) + 2\dot{\theta}\dot{u}\sin\theta + \ddot{u}\cos\theta\}\delta v$$

where,

$H_1 = 1/3 + m_T$ ; $H_2 = 33/140 + m_T$; $H_3 = 11/40 + m_T$;

$H_4 = 1/2 + m_T$ ; $H_5 = 3/8 + m_T$; $H_6 = 1 + m_T + m_R$

Substituting the virtual work contributions into eq. (A1) and setting the resulting coefficients of the variational terms, $\delta\theta$, $\delta u$, $\delta w$ and $\delta v$, to zero, yields the equations of motion. The equations of motion involve the degrees-of-freedom $\theta$, $w$, $v$, $u$ and the boom tensile load $P$. The equation of motion associated with axial motion, $\delta u$, provides the value of $P$ as,

$$P = \bar{m}_B \omega_p^2 (H_1 L\dot{\theta}^2 - H_3 w\ddot{\theta} - 2H_3 \dot{w}\dot{\theta} - H_1 \ddot{u} + H_1 \dot{\theta}^2 u - H_4 \ddot{v}\cos\theta) \qquad \text{(A6)}$$

where the right hand side of eq. (A6) is recognized as an approximation to the centrifugal force in the boom.

A simplifying assumption is now made that the boom is inextensional. To first order nonlinear terms this implies the relationship of eq. (2).

As a consequence of eqs. (A6) and (2), the equations of motion as given by eq. (3) are produced where the terms of the system mass matrix are given by,

$I_{ww} = H_2/H_1$ ; $I_{vv} = H_6/H_1$ ; $I_{vw} = H_5/H_1$ ;

$I_{\theta w} = H_3/H_1$ ; $I_{\theta v} = H_4/H_1$

Grouping the nonlinear terms in accordance with eq. (4a), the $g_i$ vectors can be written as

$$g_i = \begin{Bmatrix} g_i^{(\theta)} \\ g_i^{(v)} \\ g_i^{(w)} \end{Bmatrix}$$

where the nonzero components are

$$g_1^{(\theta)} = I_{vw}(w/L)(\ddot{v}/L)\cos\theta$$

$$g_1^{(v)} = I_{vw}[\ddot{\theta}(w/L)\cos\theta - \dot{\theta}^2(w/L)\sin\theta + 2\dot{\theta}(\dot{w}/L)\cos\theta]$$
$$-I_{\theta v}\dot{\theta}^2\cos\theta$$

$$g_1^{(w)} = -I_{ww}(w/L)\dot{\theta}^2 \qquad \text{(A7)}$$

$$g_2^{(\theta)} = I_{ww}[(w/L)^2\ddot{\theta} + 2(w/L)(\dot{w}/L)\dot{\theta}] \qquad \text{(A8)}$$

$$g_3^{(w)} = (6/5)(w/L)\dot{\theta}^2 \qquad \text{(A9)}$$

$$g_4^{(\theta)} = -(6/5)(w/L)^2\ddot{\theta}[1-(6/5)(w/L)^2]$$
$$-(3/5)I_{\theta w}(w/L)[(\ddot{w}/L)(w/L)+2(\dot{w}/L)^2]$$
$$-(12/5)(\dot{w}/L)(w/L)\dot{\theta}[1-(3/5)(w/L)^2]$$
$$+(3/5)I_{\theta v}(w/L)^2(\ddot{v}/L)\sin\theta$$

$$g_4^{(v)} = I_{\theta v}[(3/5)(w/L)^2(\ddot{\theta}\sin\theta + \dot{\theta}^2\cos\theta)$$
$$+(12/5)\dot{\theta}(\dot{w}/L)(w/L)\sin\theta$$
$$-(6/5)L\{(\ddot{w}/L)(w/L)+(\dot{w}/L)^2\cos\theta\}]$$

$$g_4^{(w)} = (18/25)(w/L)^2[2(\ddot{w}/L)-\dot{\theta}^2(w/L)+2(\dot{w}/L)^2/(w/L)]$$
$$-(6/5)I_{\theta v}(\ddot{v}/L)(w/L)\cos\theta$$
$$-(3/5)I_{\theta w}\ddot{\theta}(w/L)^2 \qquad \text{(A10)}$$

where the superscripts $(\theta)$, $(v)$ and $(w)$ refer to the degrees-of-freedom which the components of the $g_i$ vectors are associated with.

## REFERENCES


1. Tabarrok, B.;Leech, C.M.; and Kim, Y.I.: On the Dynamics of an Axially Moving Beam. Journal of the Franklin Institute, Vol.297, No. 3, pp. 201-220, March 1974.

2. Lips, K.W. and Modi, V.J.: Transient Attitude Dynamics of Satellites With Deploying Flexible Appendages. Acta Astronautica, Vol. 5, pp. 797-815, 1978.

3. Lips, K.W. and Modi, V. J.: Dynamics of a Deploying, Orbiting Beam Type Appendage Undergoing Librations. ASME Design Engineering Technical Conf., Hartford, Conn., ASME Paper No. 81-DET63, Sept. 1981.

4. Weidman, D.J. and Housner,J.M.: Assessment of Dynamic Analyses for Deploying Space Truss Structures. AIAA 25th SDM Conf., May 1984, AIAA Paper No. 84-0924-CP.

5. Ebert, K.: Dynamik Eines Satelliten mit Beweglichen Auslegern, ZAMM Journal, pg. T34T35, Vol. 62, 1981.

6. Sellappan, R. and Bainum, P.M.: The Motion and Stability of Spin-Stabilized Spacecraft With Hinged Appendages. AIAA Paper No. 76-784, Astrodynamics Conf., Aug. 1976.

7. Lang, W.E. and Honeycutt, G.H.: Simulation of Deployment Dynamics of Spinning Spacecraft. NASA TN D-4074, Aug. 1967.

8. Stoll, H.W., Jr.: Systematic Design of Deployable Space Structures, 2nd AIAA Conference on Large Space Platforms, AIAA Paper No. 81-04444, Feb, 1981.

9. Housner, J.M.: Convected Transient Analysis for Large Space Structures Manuever and Deployment. AIAA 25th SDM Conf., May 1984, AIAA Paper No. 84-1023-CP.

10. Kane, T.R.; Likens, P.W.; and Levinson, D.A.: Spacecraft Dynamics. McGraw-Hill Publishers, N.Y., 1983.

11. Hunter, J.A.; Ussher, T.H.; and Gossain, D.M.: Structural Dynamic Design Considerations of the Shuttle Remote Manipulator System. AIAA 23rd SDM Conf., May 1982, AIAA Paper No. 82-0762.

12. Housner, J.M.; and Belvin, W.K.: On the Analytical Modeling of The Nonlinear Vibrations of Pretensioned Space Structures. J. of Computers and Structures, Vol. 16, No. 1-4, pp. 339-352, 1983.

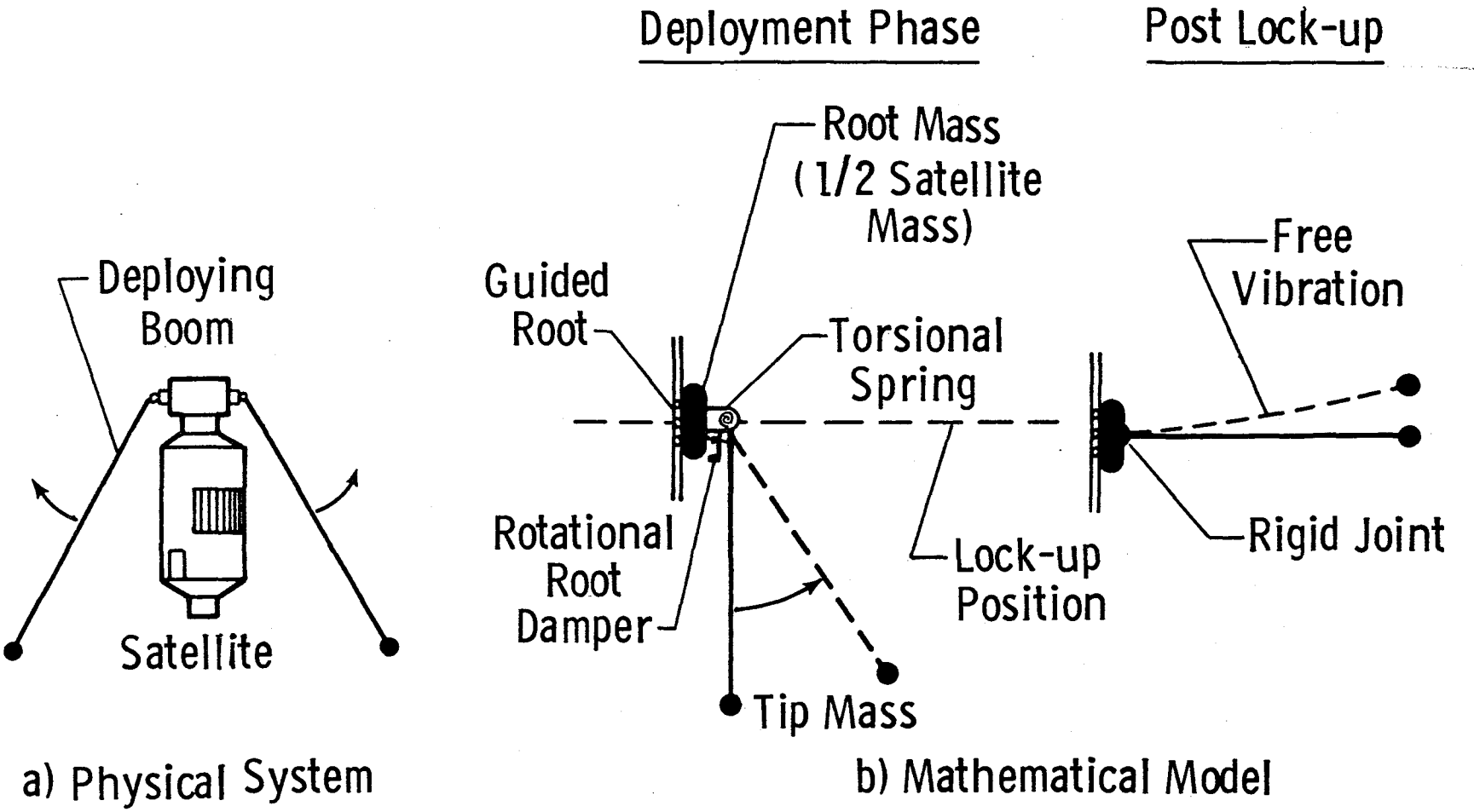


Fig. 1 Fundamental deployment problem.

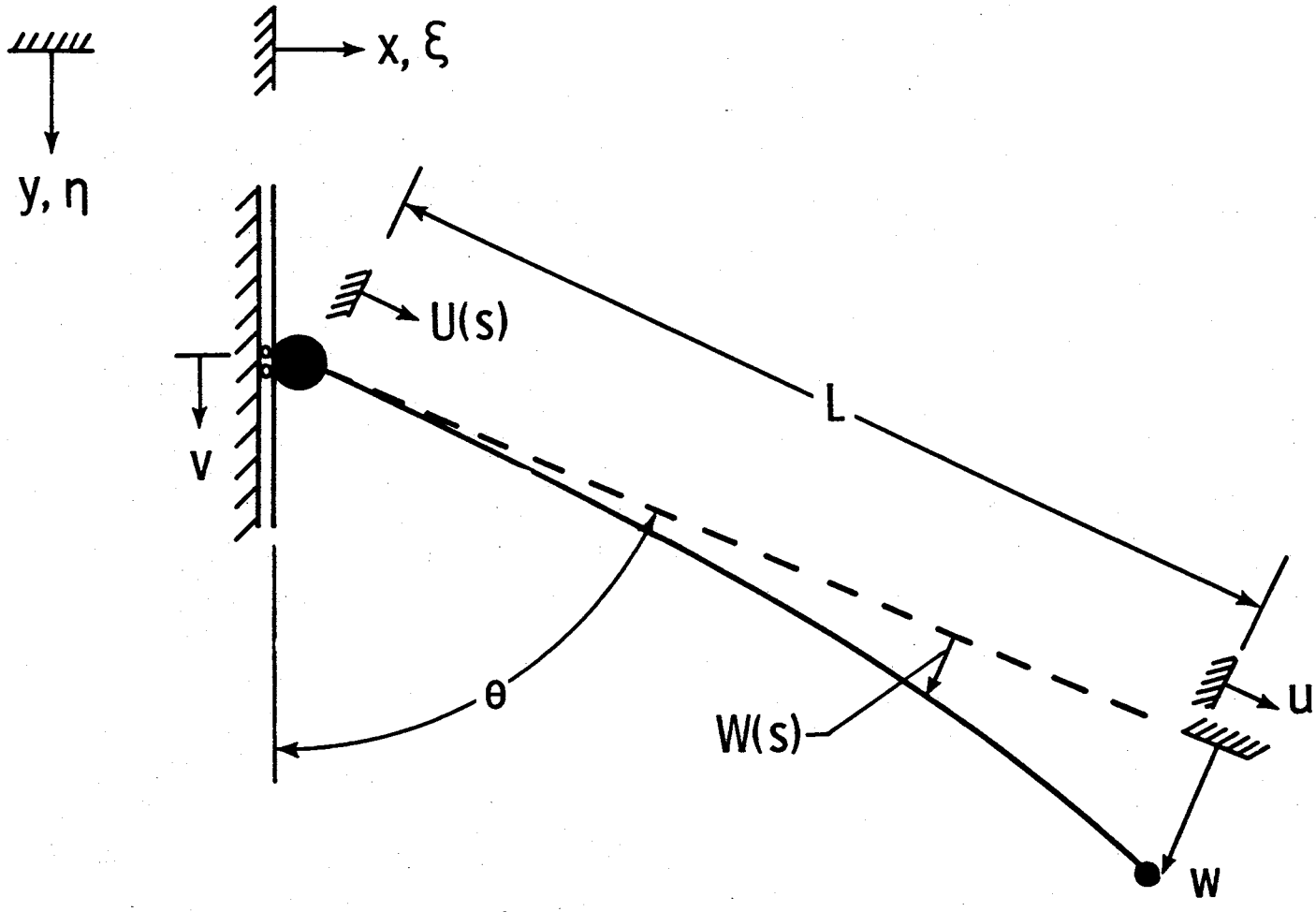


Fig. 2 Geometry and coordinate system during deployment phase.

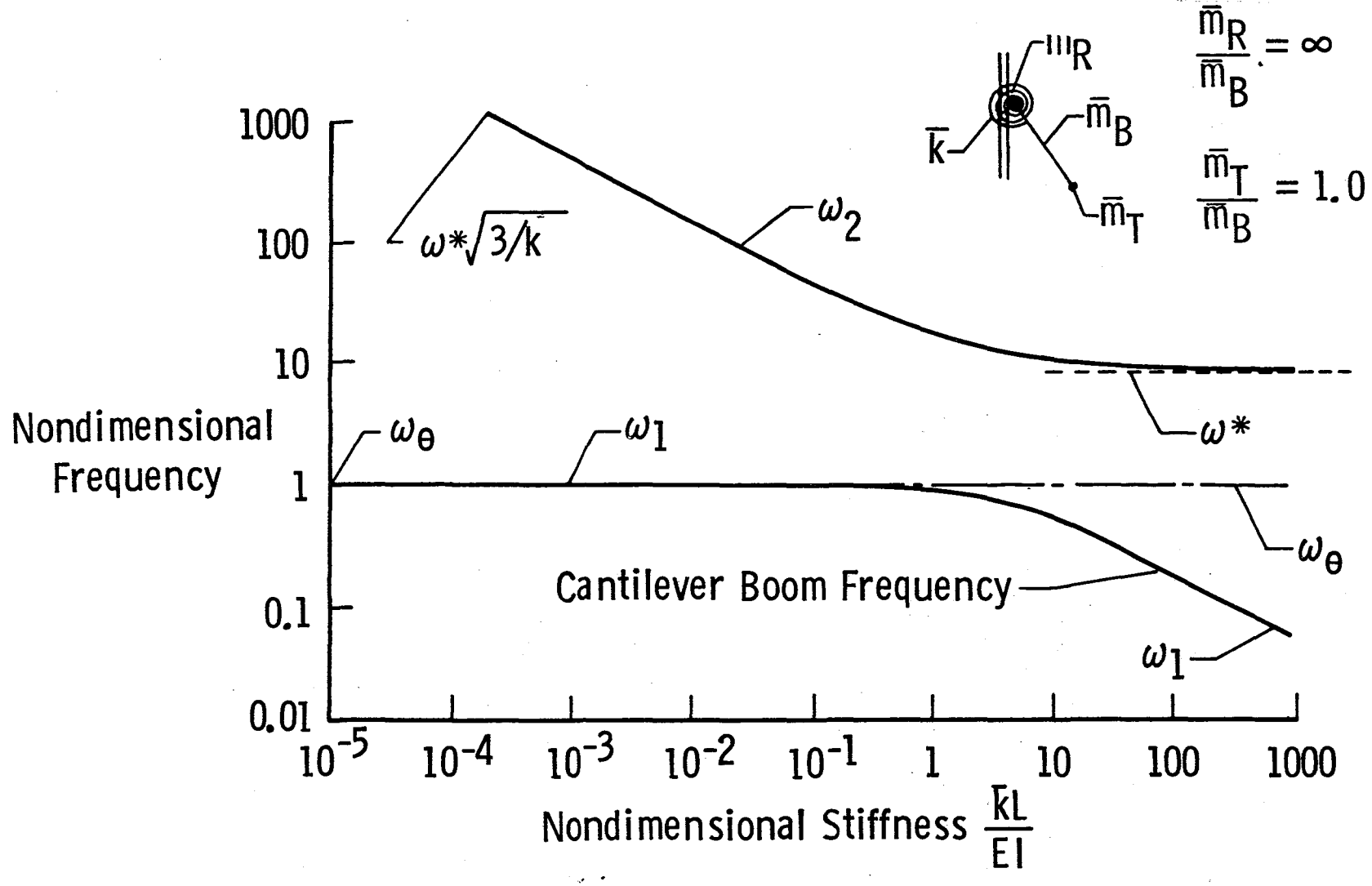


Fig. 3 Variation of nondimensional frequencies with nondimensional stiffness.

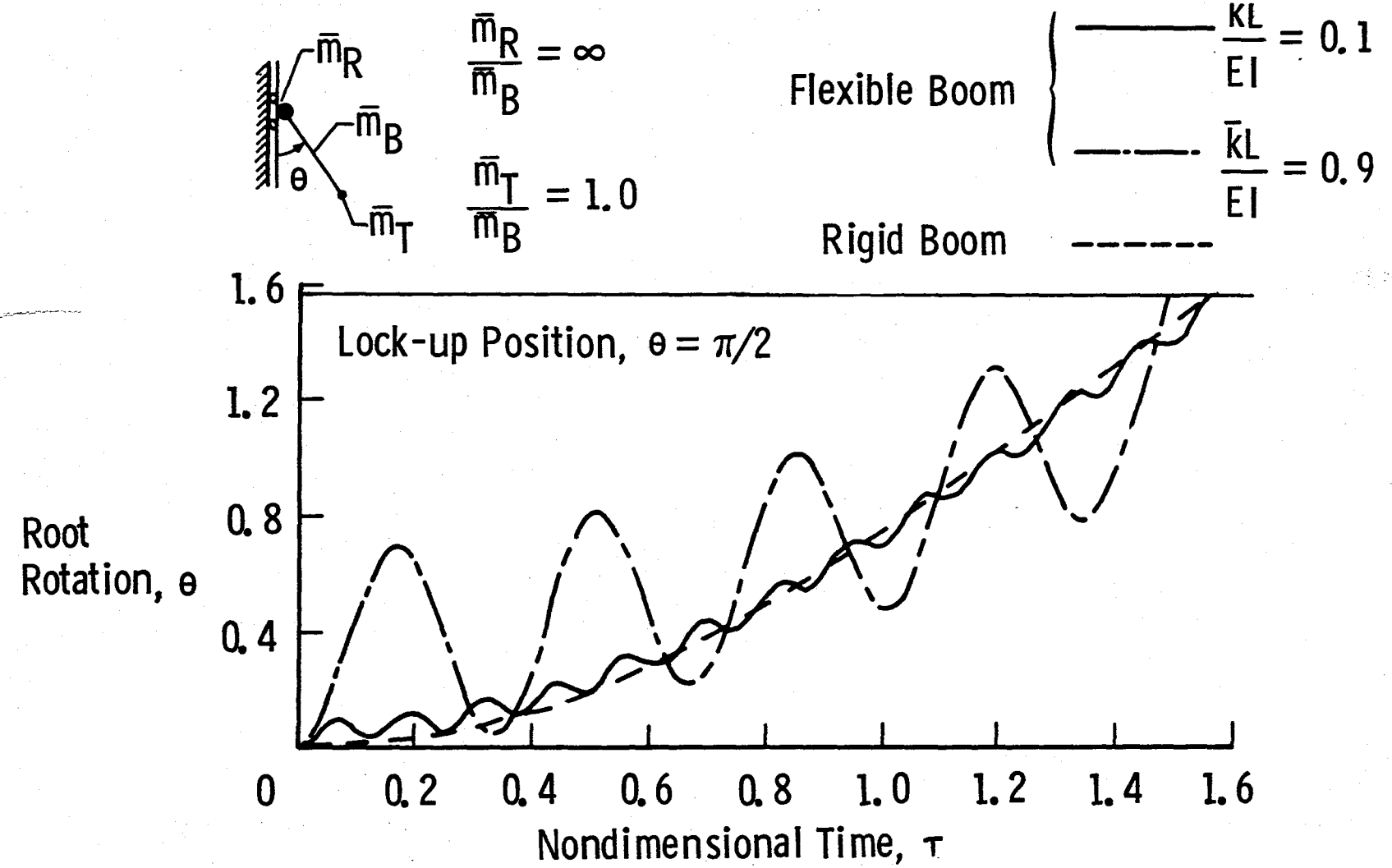


Fig. 4 Root rotation history during deployment.

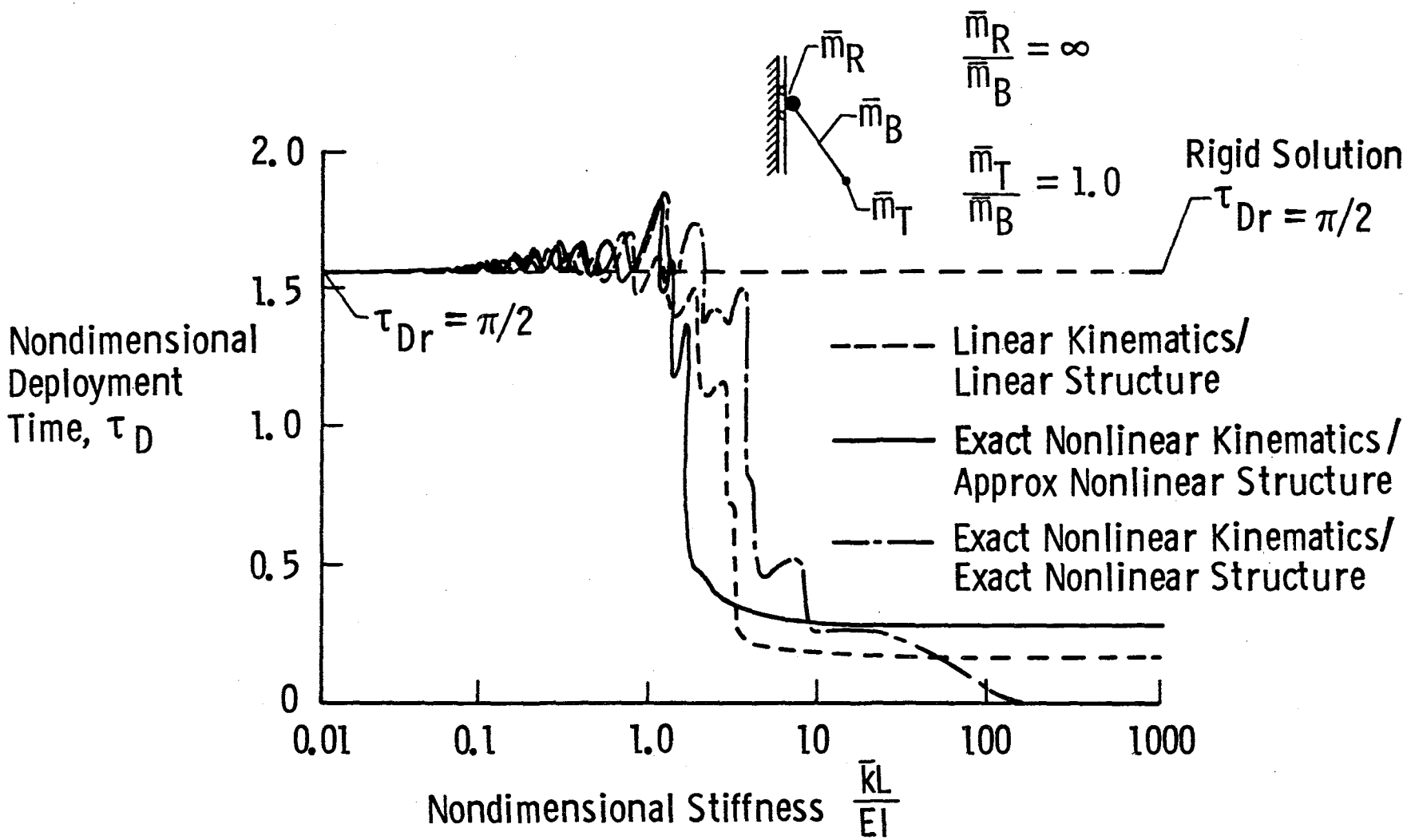


Fig. 5 Variation of nondimensional deployment time with nondimensional stiffness.

Fig. 5(a) Comparison of selected approximations with exact solution.

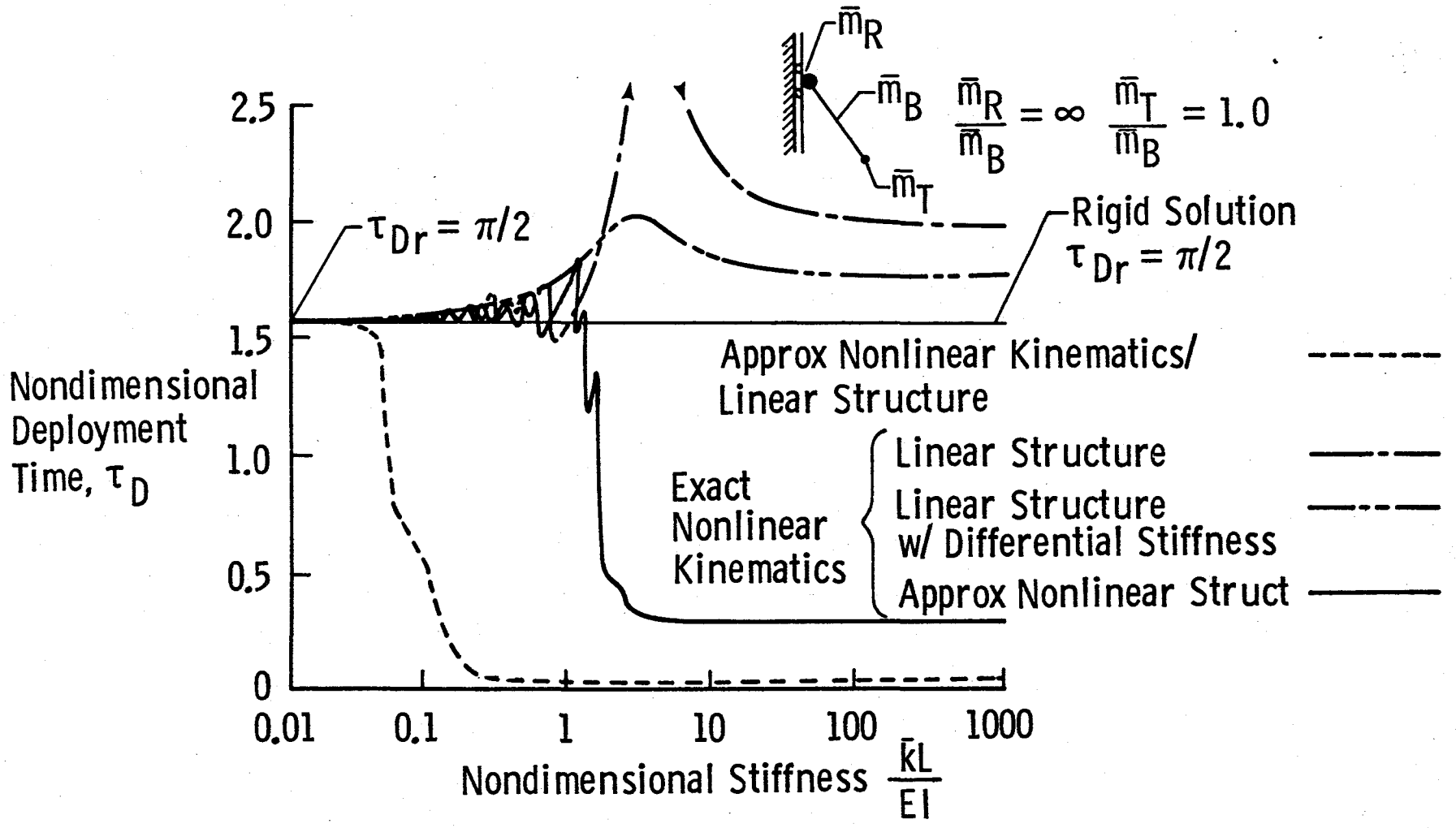


Fig. 5(b) Effect on predicted solutions to neglecting various orders of nonlinear kinematics and structural terms.

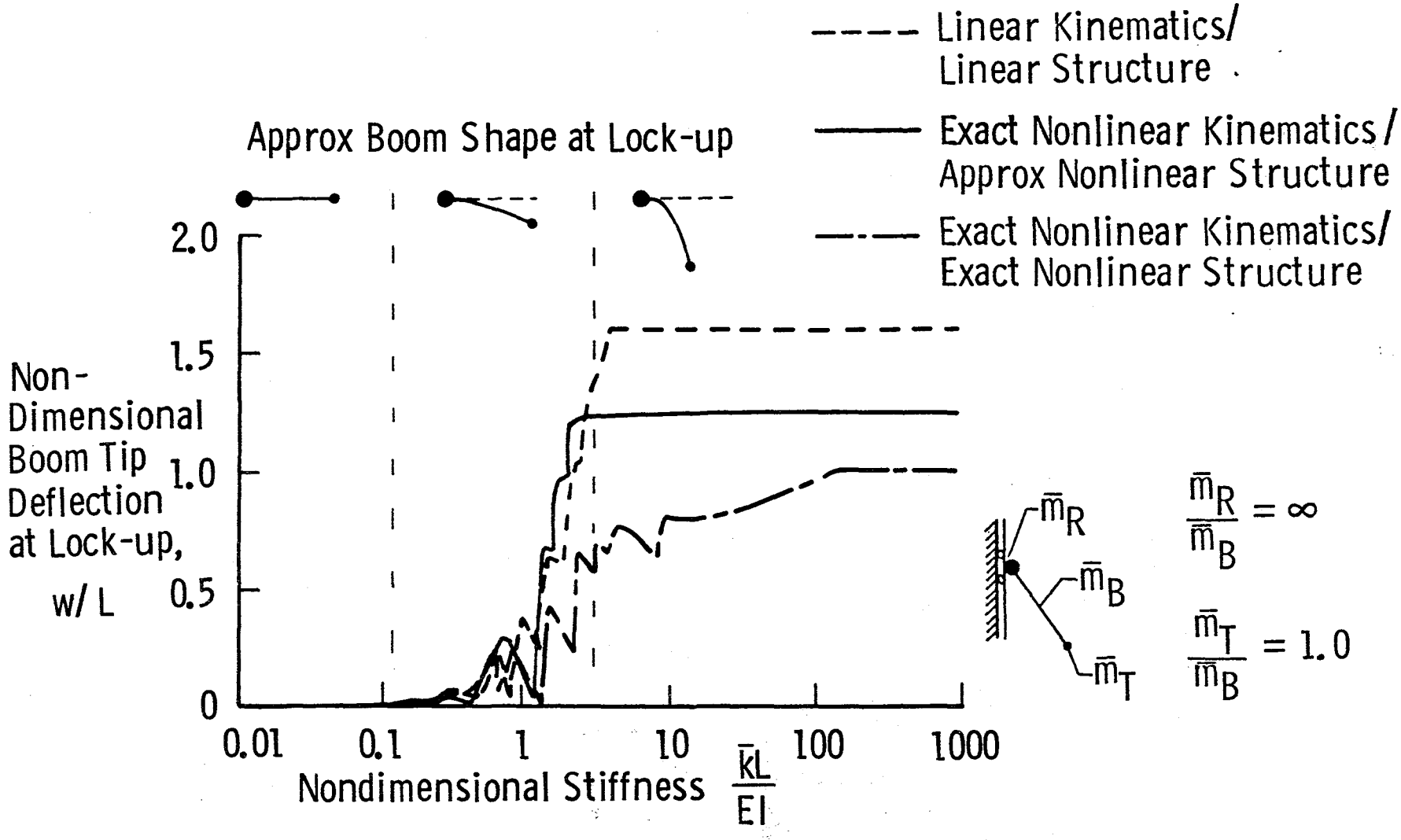


Fig. 6 Variation of boom tip deflection at lock-up with nondimensional stiffness.

Fig. 6(a) Comparison of selected approximation with exact solution.

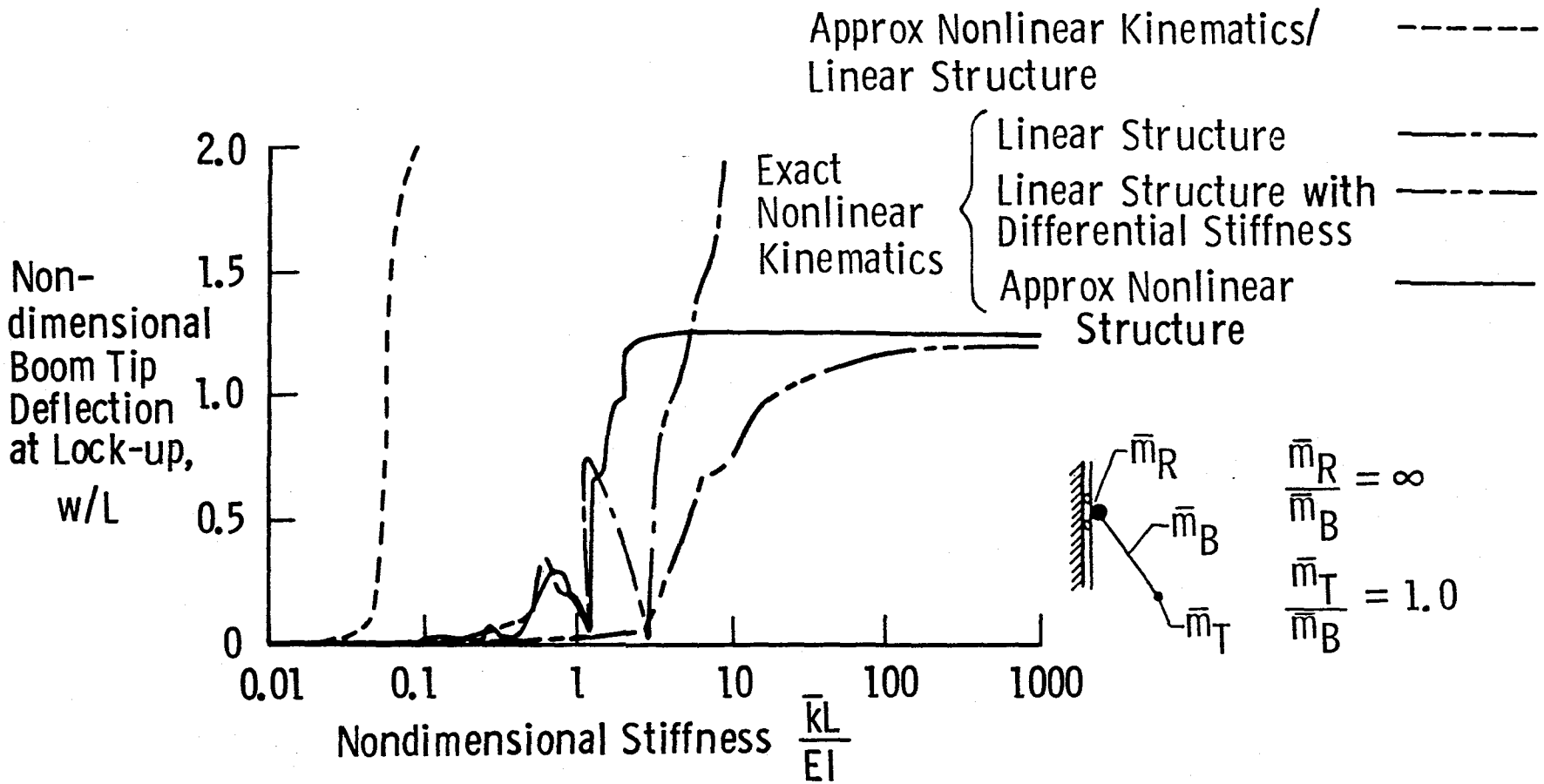


Fig. 6(b) Effect on predicted solutions to neglecting various orders of nonlinear kinematic and structural terms.

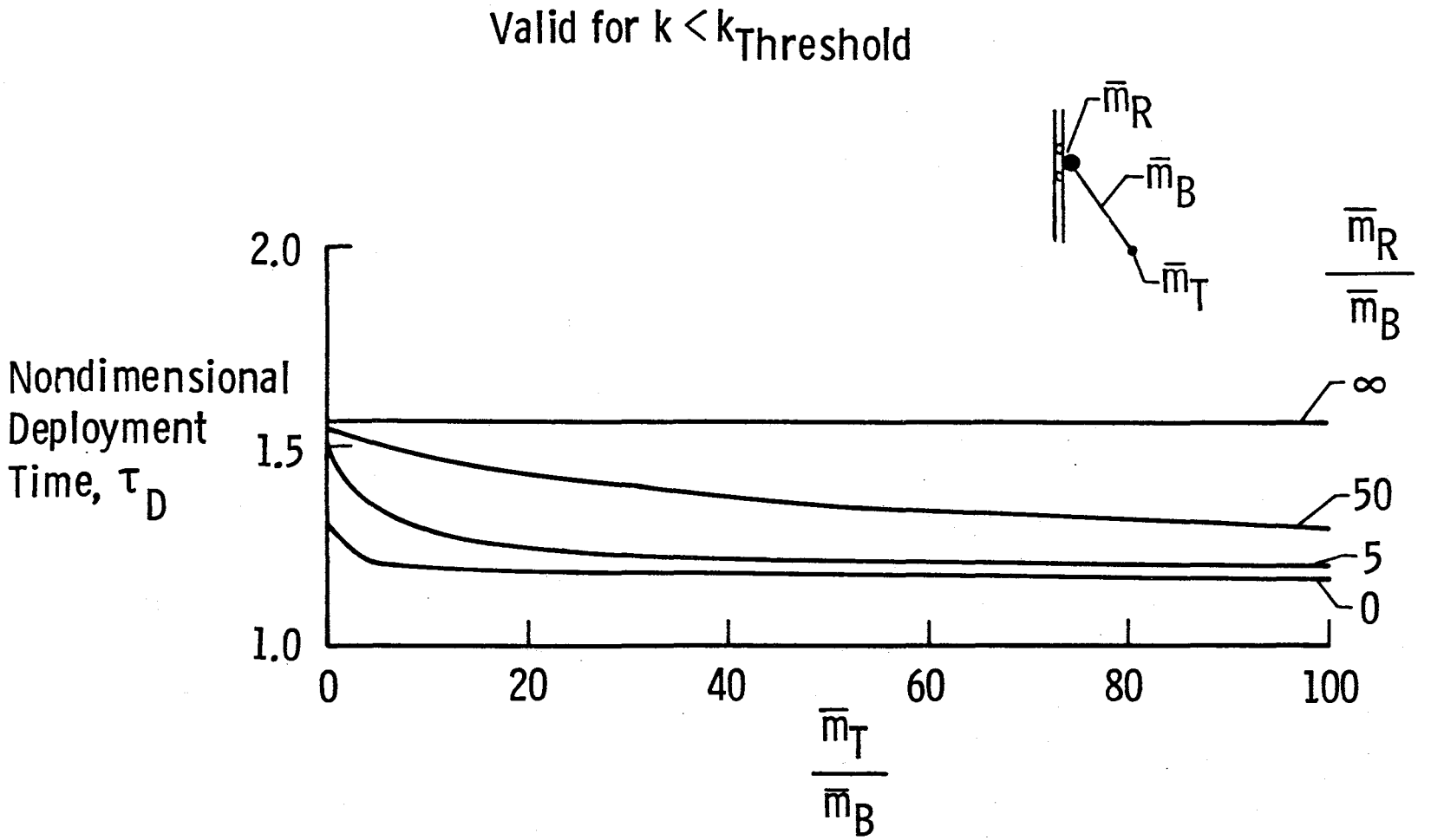


Fig. 7 Nondimensional deployment time versus mass ratios for rigid booms.

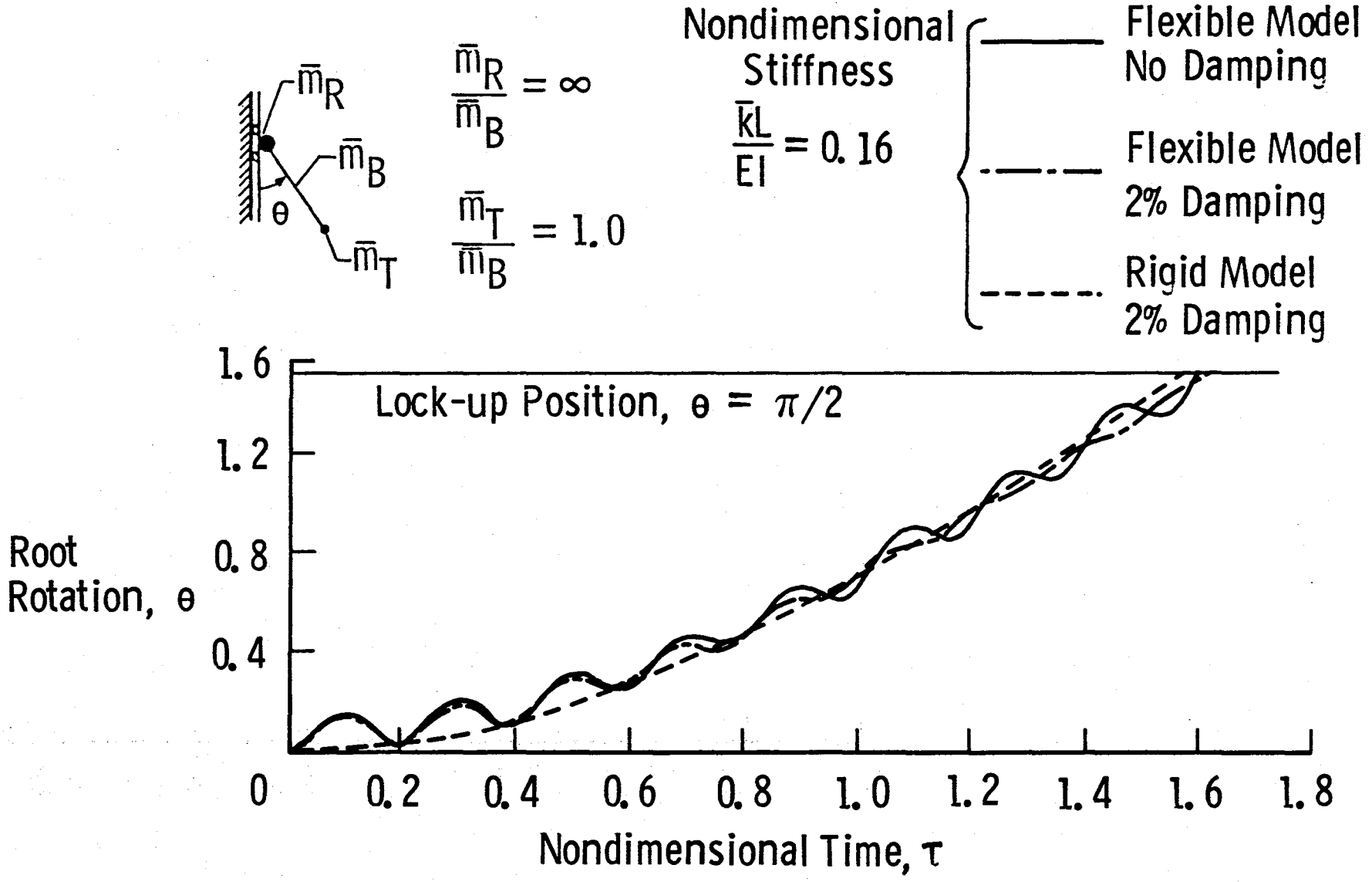


Fig. 8 Effect of root damping on boom vibrations during deployment.

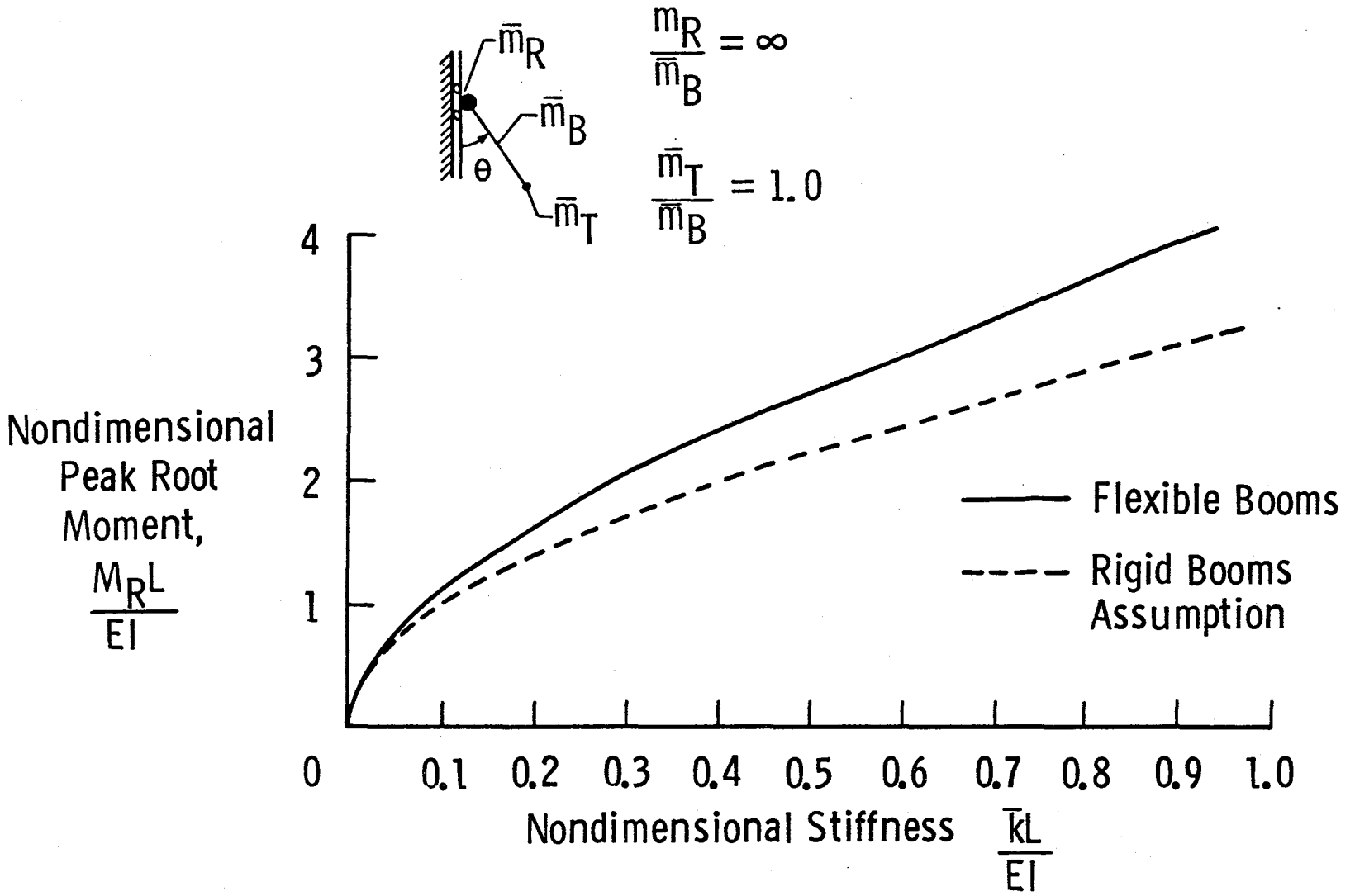


Fig. 9 Variation of post-lock-up root moments with nondimensional stiffness.

| 1. Report No. | 2. Government Accession No. | 3. Recipient's Catalog No. |
|---|---|---|
| NASA TM-87617 | | |

| 4. Title and Subtitle | 5. Report Date |
|---|---|
| Nonlinear Dynamic Analysis of Deploying Flexible Space Booms | September 1985 |
| | 6. Performing Organization Code 506-43-51-02 |
| 7. Author(s) | 8. Performing Organization Report No. |
| Paul E. McGowan and Jerrold M. Housner | |
| 9. Performing Organization Name and Address | 10. Work Unit No. |
| National Aeronautics and Space Administration<br>Langley Research Center<br>Hampton, VA 23665-5225 | 11. Contract or Grant No. |
| | 13. Type of Report and Period Covered |
| 12. Sponsoring Agency Name and Address | Technical Memorandum |
| National Aeronautics and Space Administration<br>Washington, DC 20546-0001 | 14. Sponsoring Agency Code |

15. Supplementary Notes

16. Abstract

A fundamental investigation of the planar deployment and lock-up of two flexible boom-type appendages which have attached tip masses and are connected to a central rigid body through a rotational spring is presented. Nondimensional parameters are identified and it is shown that, in general, the solution depends only on two mass ratios and one non-dimensional stiffness parameter. Results are presented for boom tip deflections, deployment time and root moments at lock-up. A threshold value of the nondimensional stiffness parameter is identified beyond which boom deflections become large. Also, a thorough examination of the effect of nonlinear terms in the equations governing the deployment phase is performed. Nonlinear terms in the deployment equations due to kinematics and structural deformation are required to predict more accurately boom deflections, but retention of an inconsistent set of nonlinear terms leads to erroneous results. In particular, retaining nonlinear kinematic terms while neglecting nonlinear structural terms can produce inaccurate results even below the threshold stiffness value.

| 17. Key Words (Suggested by Author(s)) | 18. Distribution Statement |
|---|---|
| Space Structures<br>Deployment<br>Flexible Booms<br>Nonlinear Kinematics | Unclassified - Unlimited<br>Subject Category - 39 |

| 19. Security Classif. (of this report) | 20. Security Classif. (of this page) | 21. No. of Pages | 22. Price* |
|---|---|---|---|
| Unclassified | Unclassified | 33 | A03 |



For sale by the National Technical Information Service, Springfield, Virginia 22161